Characterization of the UV detector of Solar Orbiter/Metis

Uslenghi, Michela, Schühle, Udo, Teriaca, Luca, Heerlein, Klaus, Werner, Stephan

Michela Uslenghi, Udo H. Schühle, Luca Teriaca, Klaus Heerlein, Stephan Werner, "Characterization of the UV detector of Solar Orbiter/Metis," Proc. SPIE 10397, UV, X-Ray, and Gamma-Ray Space Instrumentation for Astronomy XX, 103971K (29 August 2017); doi: 10.1117/12.2274944

SPIE.

Event: SPIE Optical Engineering + Applications, 2017, San Diego, California, United States

Characterization of the UV detector of Solar Orbiter/Metis

Michela Uslenghi[*a], Udo H. Schühle[b], Luca Teriaca[b], Klaus Heerlein[b], Stephan Werner[b]

[a]INAF - IASF Milano, Via Edoardo Bassini 15 20133 (Italy); [b] Max Planck Institute for Solar System Research, Justus-von-Liebig-Weg 3, 37077 Göttingen (Germany)

ABSTRACT

Metis, one of the instruments of the ESA mission Solar Orbiter (to be launched in February 2019), is a coronograph able to perform broadband polarization imaging in the visible range (580-640 nm), and narrow band imaging in UV (HI Lyman-α 121.6 nm) . The detector of the UV channel is an intensified camera, based on a Star-1000 rad-hard CMOS APS coupled via a 2:1 fiber optic taper to a single stage Microchannel Plate intensifier, sealed with an entrance MgF_2 window and provided with an opaque KBr photocathode. Before integration in the instrument, the UVDA (UV Detector Assembly) Flight Model has been characterized at the MPS laboratory and calibrated in the UV range using the detector calibration beamline of the Metrology Light Source synchrotron of the Physikalisch-Technische Bundesanstalt (PTB). Linearity, spectral calibration, and response uniformity at 121.6 nm have been measured. Preliminary results are reported in this paper.

Keywords: UV detectors, Solar Orbiter, MCP, APS

1. INTRODUCTION

Solar Orbiter [1] will provide the next major step forward in the exploration of the Sun and the heliosphere after the successful ESA missions Ulysses and SOHO, as well as the NASA missions TRACE, RHESSI, STEREO and SDO and JAXA mission Hinode. Solar Orbiter is a mission of ESA's Cosmic Vision program and a key element of NASA's *International Living with a Star* program, which is focused on the objective of understanding the governing processes of the connected Sun-heliosphere system.

Thanks to the powerful combination of in-situ and remote-sensing instruments and the unique inner-heliospheric mission orbit design, Solar Orbiter will address the central question of how the Sun creates and controls the heliosphere. In fact, Solar Orbiter will approach the Sun to within 0.28 AU, leading also to high resolution observations of the regions magnetically linked to the spacecraft. Moreover, its orbit out of the ecliptic plane will allow an unprecedented close-up views of the Sun's polar regions at solar latitudes higher than 30º. This proximity to the Sun will also give the advantage of flying with an angular velocity significantly closer to that of Sun's rotation than the angular velocity of the Earth at 1 AU, allowing observations of both the on-disk inner corona and the outer corona for a significantly longer temporal interval than as seen from ground.

The coronagraph Metis, one of the ten (and one of the six remote-sensing) instruments on board, will provide the capability of investigating the Sun corona in the visible and UV (121.6 nm) range.

1.1 Metis

The Metis coronagraph, based on a on-axis Gregorian telescope with an innovative design to minimize the thermal load [2][3], is designed to perform coronagraphic multi-wavelength imaging with unprecedented (for a space born coronagraph) temporal and spatial resolution (down to 4000 km). It will allow the study of the structures and dynamics of the full corona in the field-of-view (FOV) from 1.5º to 2.9º, corresponding to a range from 1.6 to 3.0 solar radii ($R_\odot$)

[*]uslenghi@iasf-milano.inaf.it; phone +39 02 23699460; fax +39 02 2666017

UV, X-Ray, and Gamma-Ray Space Instrumentation for Astronomy XX, edited by Oswald H. Siegmund,
Proc. of SPIE Vol. 10397, 103971K · © 2017 SPIE · CCC code: 0277-786X/17/$18 · doi: 10.1117/12.2274944

at minimum perihelion (0.28 AU), and from 2.8 to 5.5 $R_\odot$ at 0.5 AU. In particular, Metis will be capable of obtaining for the first time simultaneous imaging of the full corona in:

- linearly polarized visible-light (580-640 nm)
- narrow-band ultraviolet HI Lyman-α (121.6 nm)

with high temporal cadence (up to 1 s in visible-light; up to 5 min. in the UV), and pixel size (20 arcsec in the UV, and 10 arcsec in the visible).

These measurements will allow a characterization of the main physical parameters (i.e., density, temperature, and outflow velocities) of the two most important plasma components of the corona and the solar wind (electrons and protons).

The detector assemblies for the two channels are provided by the Max-Planck-Institut für Sonnensystemforschung (MPS) of Göttingen, Germany:

- the VLDA (Visible Light Detector Assembly) is based on a custom Active Pixel Sensor (APS) developed by CMOSIS [4] and MPS, the same sensor used in another Solar Orbiter instrument *(Polarimetric and Helioseismic Imager* - PHI) [5]. The detector is a 2k x 2k array with 10 µm pixel size, digitized with 14 bit resolution.
- the UVDA (UV Detector Assembly) is an intensified APS [6], based on a Star1000 device [7], providing a 1k x 1k array with 30 µm pixel size.

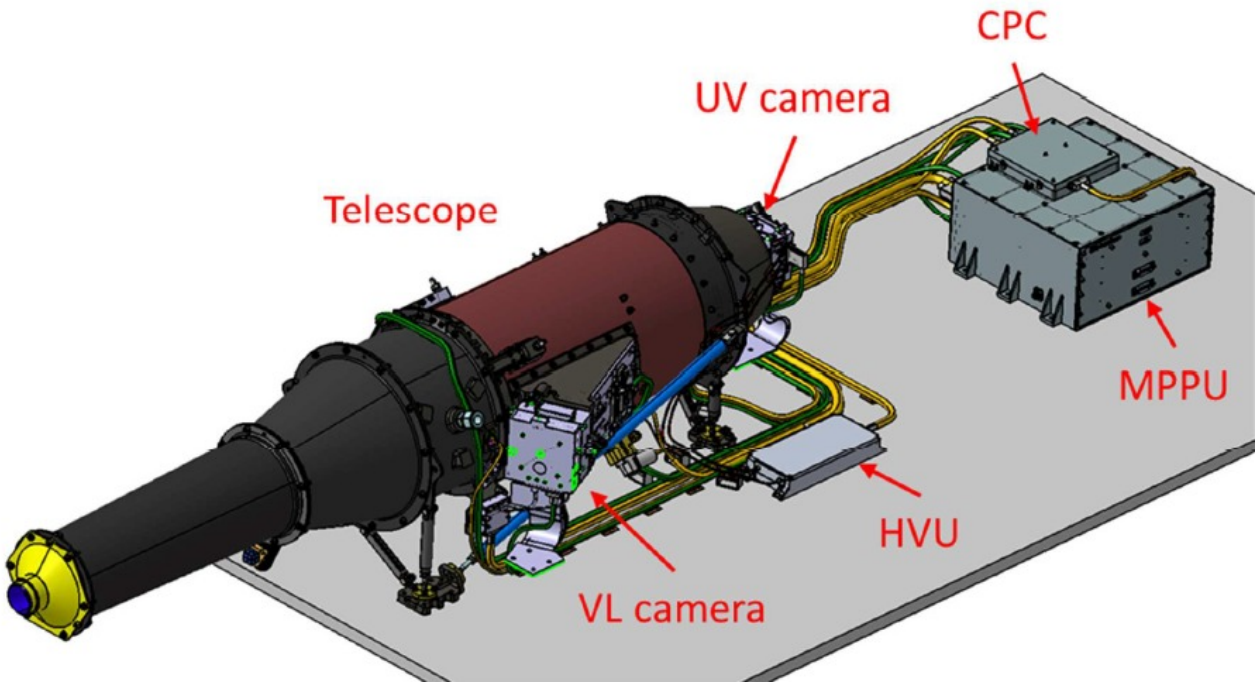

Figure 1. Metis instrument configuration, showing the location of the UVDA.

1.2 Metis UVDA

The UVDA is located within the Metis Optics Unit (MOU) and contains one intensified camera that acquires images in the Lyman alpha line of hydrogen at 121.6 nm. It is based on a 1k x 1k Star1000 APS sensor that runs up to a frame rate of 10 fps. The sensor is mated via a fiber optic taper to a single stage MCP intensifier whose front entrance is sealed by a MgF_2 window. Incoming UV photons extract electrons at the photocathode, a KBr layer deposited on the entrance face of the MCP. The electrons are then accelerated by the voltage applied between the MCP and a phosphor screen that emit a pulse of visible light photons as output. The visible light is finally channeled down to the APS sensor by the fiber optic taper. The taper is rescaling the image of the camera focal plane (i. e., the entrance of the MCP) so to match the size of

the sensor. In the case of the UVDA the scaling is 2:1, thus the 15 µm pixel size of the Star1000 translates into an effective 30 µm sampling element at the focal plane.

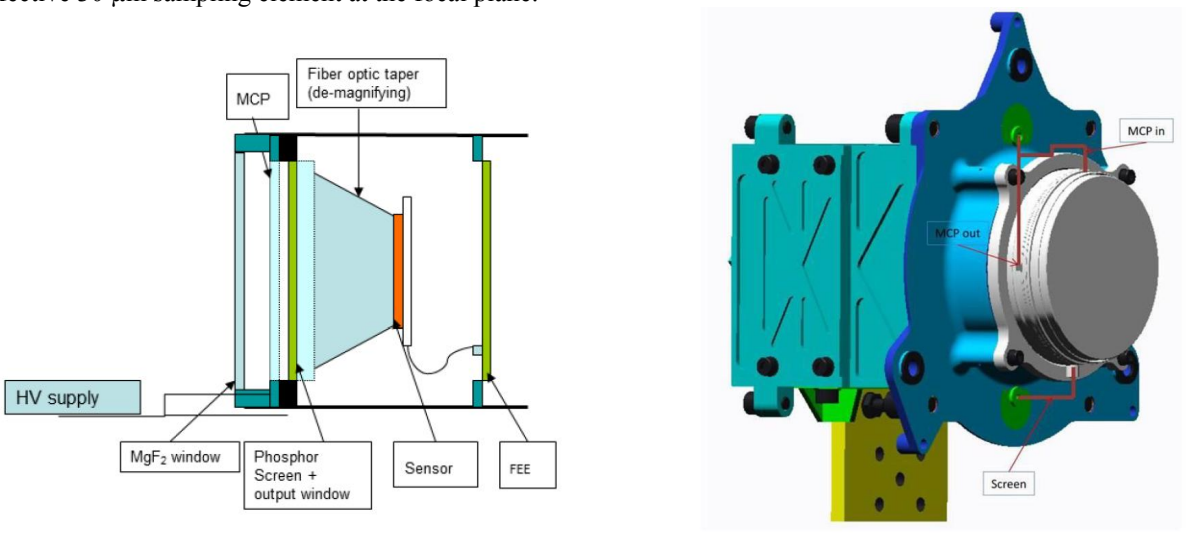

Figure 2. IAPS scheme (left) and 3D model of the UVDA (right).

Data from the camera is transferred via a channel link interface to the Metis Power and Processing Unit (MPPU) and a separate SPI interface is used for commanding and housekeeping. The power is provided by the MPPU through a Camera Power Converter (CPC), which converts the primary output voltage from the MPPU to the supply voltages for the VLDA and UVDA cameras. The voltages required by the MCP and the phosphor screen are provided by a High Voltage Unit (HVU) mounted on the S/C panel at the side of the Metis telescope. Figure 2 shows a block diagram of Metis electronics system.

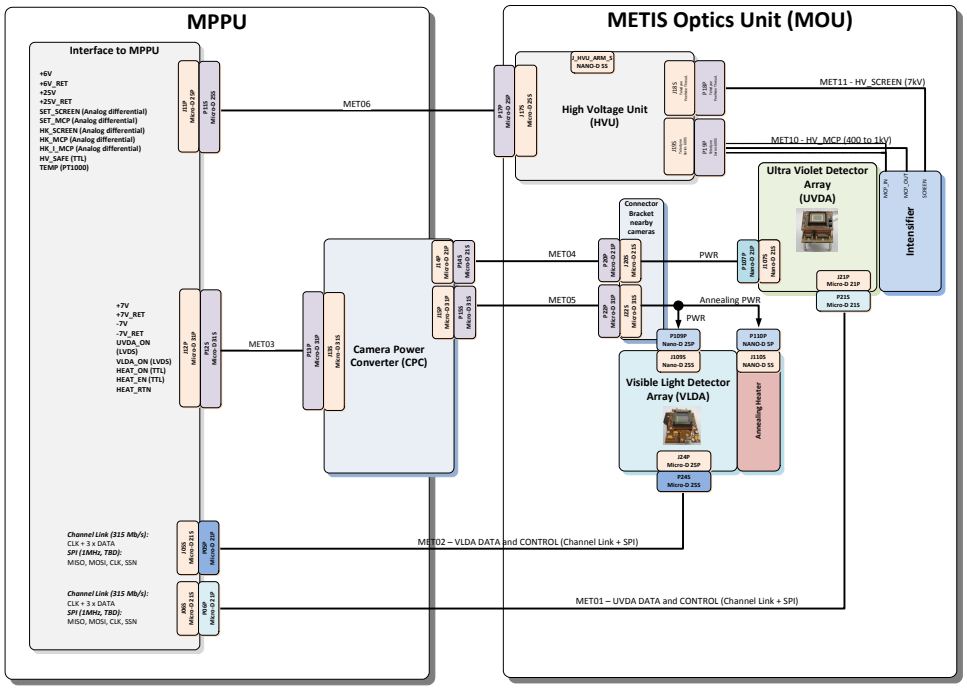

Figure 3. Metis UVDA and VLDA Electronics Block Diagram.

If the intensifier is operated at a high enough gain, it can virtually convert each primary photoelectron into a luminous spot on the phosphor screen that preserves the location of the event. Reading out the APS at the fastest frame rate (to avoid spots overlapping) it can be possible to detect the footprint of each event. A high speed digital processing electronics unit is thus needed in order to process in real time the high amount of data generated by the digital camera, without limiting the detector dynamic [7]. A single stage MCP intensifier is not optimal for photon counting due to both the low gain and the fact that it cannot operate in saturated regime. When the MCP intensifier operates in saturation, the Pulse Height Distribution (PHD) of the signals generated by incident photons has a quasi-gaussian shape [9]. Thus the signal can be easily discriminated from the noise, which has a PHD with negative exponential shape. Instead, in linear regime, the signal PHD has the same shape of the noise, making the choice of the threshold more difficult.
However, a photon counting mode has been implemented for Metis since it can be convenient with low photon flux (e.g. for observations far from the Sun or at the end of life of the mission, when the efficiency of Metis could be degraded). Centroiding the events will also allow a better spatial resolution.

In photon counting mode, the MCP intensifier is powered with voltages higher than a threshold and the APS is read out at the maximum frame rate, i. e. 10 frame/s. The output is serially acquired as to generate a 3x3 pixel^2 event window that sweeps dynamically the APS matrix. Each window is analyzed looking for the presence of events whose charge content lies within proper limits and satisfies a given set of morphological rules. The centroid coordinates of identified events are determined and subsequently sent to the MPPU as a packet containing coordinates and collected photo-charge information. For each event the MPPU receives a 32-bits packet containing: x coordinate @ 10 bits; y coordinate @ 10 bits; integrated charge amplitude@ 8 bits; morphology/quality + service info @ 4 bits. All the processing is done in real time as the camera generats the frame by a unit (Photon Counting Unit – PCU) implemented in FPGA of the MPPU.

2. EXPERIMENTAL SETUP

The UVDA FM has been characterized and calibrated, before being integrated in Metis, using facilities at MPS (for measurements not requiring continuous spectrum or calibrated sources) and at the Physikalisch-Technische Bundesanstalt (PTB) in Berlin.
A special vacuum chamber (DeKaKa) was built at MPS expressly for the characterization of all the UVDA units (namely: Qualification Model-QM, Flight Model-FM and Flight Spare-FS). The chamber can host the UVDA and the HVU, can be evacuated down to 10^{-7} hPa and has provisions for cooling the UVDA by liquid nitrogen. The chamber is transportable and it can be moved and mounted both to VUV sources at MPS and at the synchrotron beam line at PTB.

2.1 Setup at MPS

For characterization at 121.6 nm the chamber was mounted to the MPS reflectometer facility that is equipped with a Lyman alpha source (Type: Resonance HHe-LM-L). Several optical setups have been used, with different distances between the light source and the detector, to produce high intensity, quasi-flat irradiation of the full detector area. The best flat field result was obtained by placing the light source at a distance of about 90 cm away from the detector and by a pinhole stopping the source size down to 1 mm. Additionally, a Lyman alpha filter was placed on front of the source to improve the spectral purity of the beam.

2.2 Setup at PTB

The calibration of the spectral radiometric response was carried out at the Metrology Light Source (MLS) of the electron storage ring of Physikalisch-Technische Bundesanstalt (PTB) in Berlin. The MLS provides monochromatized synchrotron radiation for a beam line dedicated specially for the radiometric calibration of detectors with traceability of the radiometric quantities to a primary detector standard (a cryogenic electrical substitution radiometer) [7].
The UVDA was transported to Berlin in the DeKaKa-chamber and mounted at the beamline for detector characterizations of the MLS. In this setup, the detector is about 30 cm away from the MLS focus, where the size of the beam is approximately 1 mm x 3 mm, and the DeKaKa-chamber can be moved horizontally and vertically under vacuum relative to the MLS beam. In this way the MLS beam can be positioned at any place of the detector, providing raster scan capability across the active area.

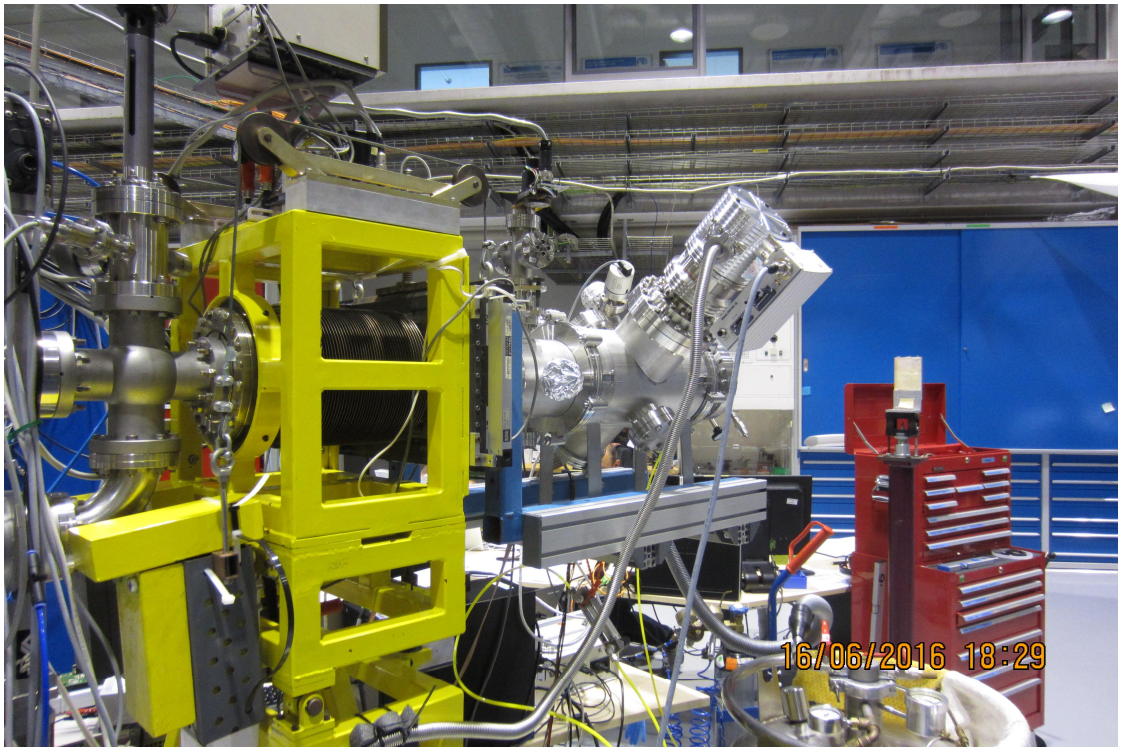

Figure 4. The DeKaKa vacuum chamber, hosting the UVDA, mounted at the beamline for detector characterizations of the MLS.

3. PRELIMINARY RESULTS

The tests carried out include the following:

- Dark current as a function of the temperature
- Linearity of the response as a function of the exposure time
- Linearity of the response as a function of the incoming flux
- Spectral radiometric calibration
- Gain as a function of the voltage applied to the MCP
- Gain as a function of the voltage applied to the gap between MCP and phosphor screen
- Response uniformity across the active area

3.1 Dark current

The nominal range of temperatures for science operation of the UVDA is [-35°C, -5°C]. The dark current of the APS has been measured for three different temperatures covering the range. The dark current of the detector is essentially due to the CMOS sensor.

The dark signal versus integration time is linear (see Fig. 5), but deviation from linearity is present at the shortest exposures. This behavior is also apparent in measurements under illumination at low signals. It is likely due to the response of the on-chip electronics and in principle can be corrected for.

The dark current increases of about 50% over 30 °C, from the lowest to the highest end of the operative range.

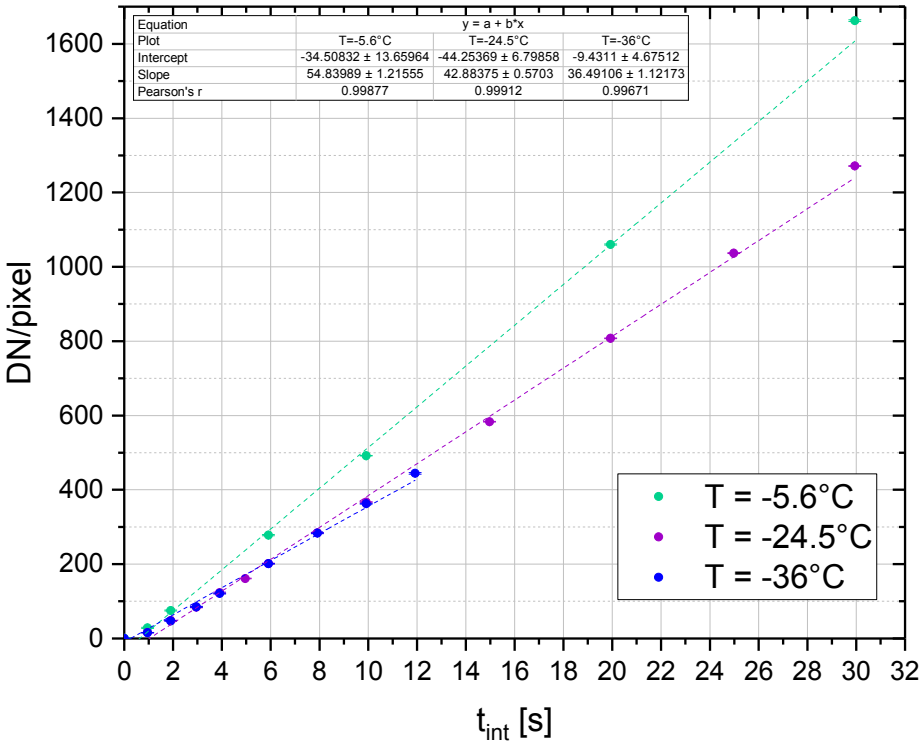

Figure 5. Dark signal vs exposure time for different temperatures.

3.2 Linearity vs flux

The linearity of the response has been tested at PTB, both as a function of the beam power and as a function of the exposure time.
The response as a function of the beam power has been measured under the conditions summarized below:

V_{MCP}	500 V
V_{SCREEN}	6000 V
λ	121.6 nm
P_{beam}	0.013-3.31 nW
T	-20°C

The beam power has been monitored with a calibrated detector.

For each data point, 40 frames have been acquired, along with 100 dark frames under the same conditions, used for dark (and bias) correction. After averaging the frames corrected for the dark, the signal of the beam as seen by the UVDA has been measured by integrating the signal over the area covered by the beam.

Figure 6 shows the results as a function of the beam power and the linear fit. Right panel shows the relative fit residuals. Deviations up to 12% with respect to the overall linear fit are present at low signals.

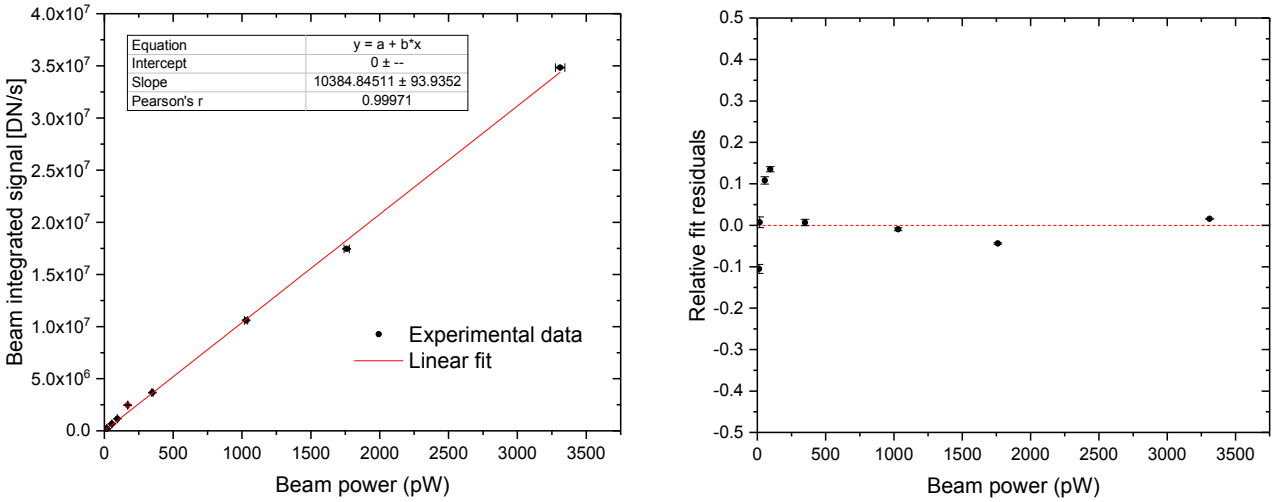

Figure 6. Output signal vs input flux (left) and related residuals from linear fit (right).

3.3 Linearity vs exposure time

The response as a function of the exposure time has been measured under the conditions summarized below:

V_{MCP}	500 V
V_{SCREEN}	6000 V
λ	121.6 nm
P_{beam}	17.5-20 pW
Integration times	1-25s
T	-20°C

The test has been carried out similarly to the previous one (40 frames for each data point, same set of darks). The beam power was slightly drifting during the measurements but the data have been corrected using the values provided by the calibrated detector that was monitoring the beam. Results are shown in Figure 7.

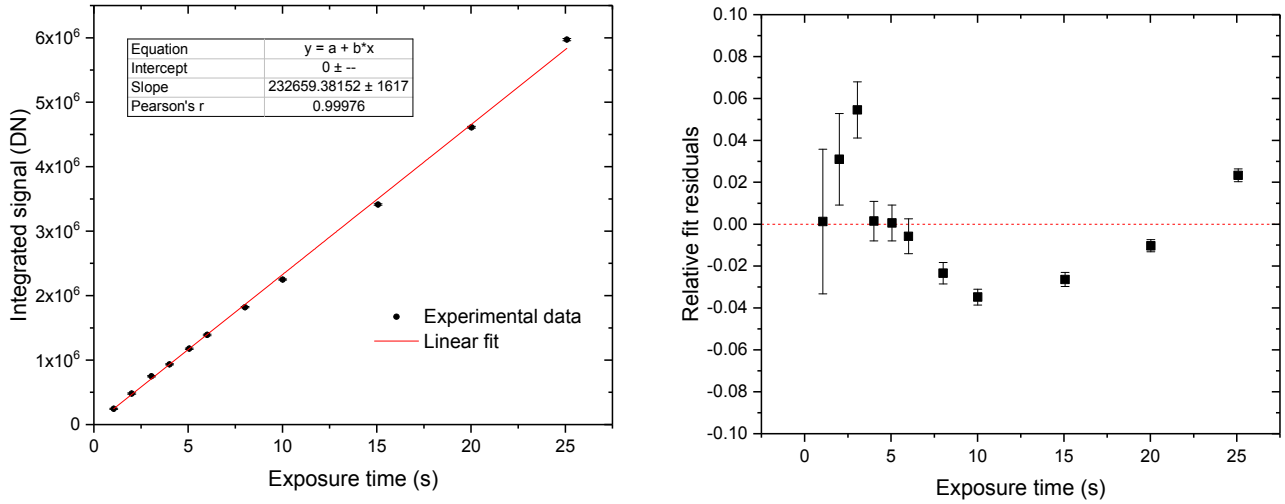

Figure 7. Output signal vs exposure time (left) and related residuals from linear fit (right).

3.4 Efficiency

Quantum efficiency, intended as the fraction of incident photons (on the camera entrance window) detected by the system, cannot be measured directly in the final detector configuration. Instead, a calibration relationship between the incident photon flux and the output signal in DNs, for the various voltage settings of the intensifier MCP and phosphor screen and for the established sensor gain, can be established.

Spectral calibration provides measurements of the product of 5 terms:

$$\eta(\lambda, V_{MCP}, V_{screen}) = QE_{photocathode}(\lambda) \times Gain_{MCP}\,(V_{MCP}) \times Gain_{Phosphor}\,(V_{screen}) \times QE_{APS} \times Gain_{APS.}$$

Since each term of the product depends on one single parameter, it is possible to characterize the dependence on each parameter separately.

The relationship between the incident photon flux and the output signal in DN has been measured and characterized as a function of:

- Wavelength λ
- MCP voltage V_{MCP}
- Phosphor screen voltage Vscreen

Effect of different temperatures has also been tested.

3.4.1 Spectral calibration

The response has been characterized at PTB-MLS between 115 and 310 nm. Two sets of measurements have been taken at different temperatures:

	Set 1	**Set 2**
V_{MCP}	400 V	400 V
V_{SCREEN}	6000 V	6000 V
λ	115-310 nm	115-300 nm
P_{beam}	0.17-2340 nW	0.42-2820 nW
Integration times	1 s - 30 s	1 s - 20 s
T	0 °C	-20 °C

A set of 40 frames + 40 dark frames have been acquired for each data point. The resulting plot is shown in Figure 8.

At higher temperature, the efficiency seems significantly higher (Figure 9), but the dependence on the wavelength is similar between the two measurements.

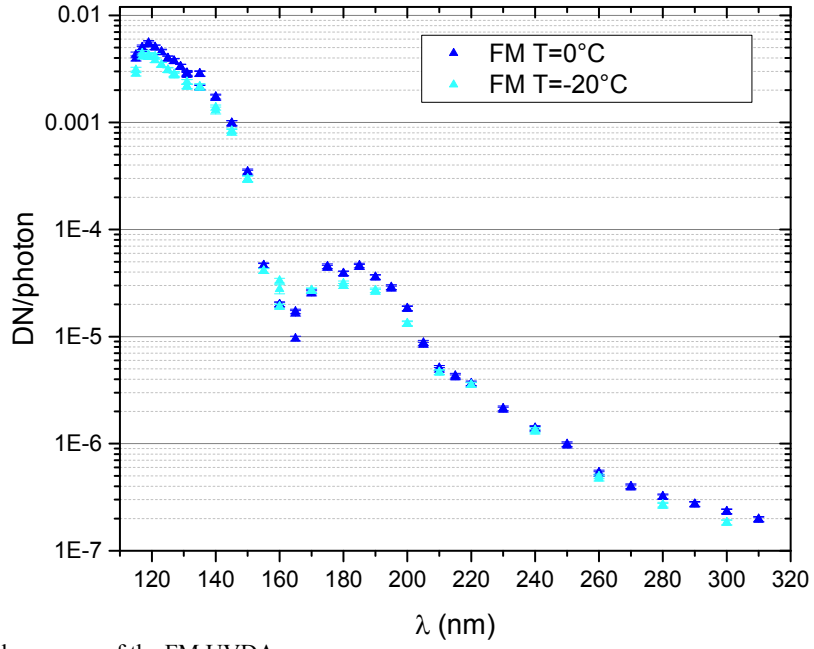

Figure 8. Spectral response of the FM UVDA.

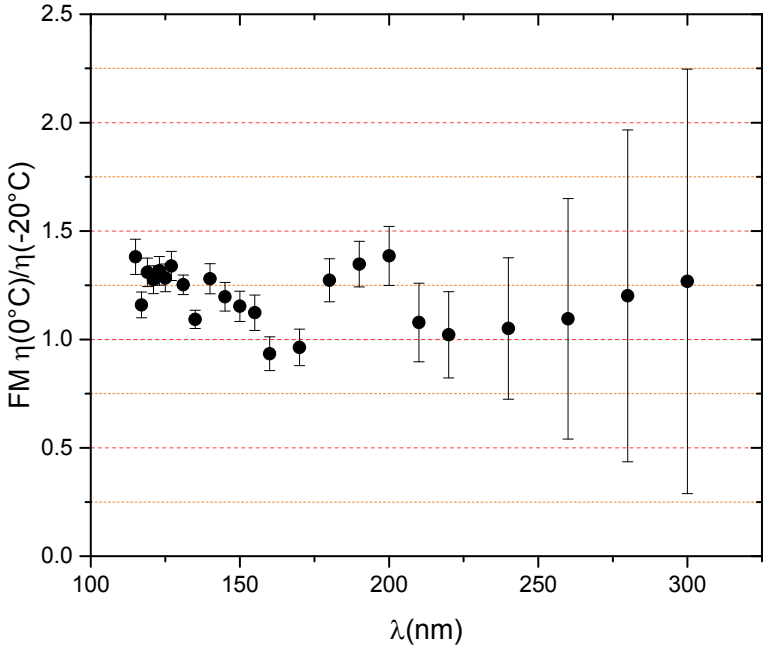

Figure 9. Ratio of efficiency vs wavelength at 0 °C and -20 °C.

3.4.2 Gain vs MCP voltage

The gain of the intensifier has been characterized as a function of the voltage applied to the MCP using a fixed screen voltage of 6000 V and under illumination with 121.6 nm light.

The conditions of the test are summarized below:

V_{MCP}	300 V - 1000 V
V_{SCREEN}	6000 V
λ	121.6 nm
P_{beam}	0.6 pW - 188 pW
Integration times	0.01 s – 40 s
T	-20 °C

The gain as a function of the voltage, normalized to the gain at 400 V (see green lines for reference), is shown in Figure 10. The absolute values on the right axes have been derived from the spectral calibration. The dependence on V_{MCP} is close to an exponential for most of the range explored, but with some significant deviation at low and high voltages. At the given input intensity, the gain saturation starts setting in at 800 V.

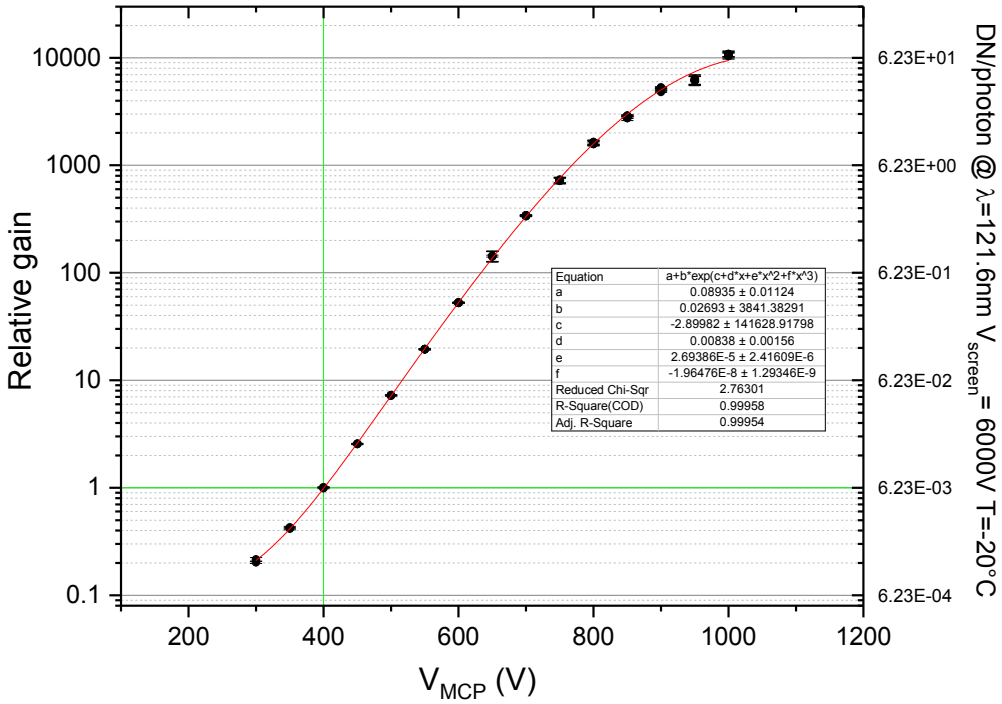

Figure 10. Relative gain vs MCP Voltage. The screen voltage was set to 6000 V.

3.4.3 Gain vs screen voltage

The gain of the intensifier has been characterized as a function of the voltage applied to the gap between the MCP and the phosphor screen using a fixed MCP voltage of 400 V and under illumination with 121.6 nm light.

The output signal (Figure 11) increases linearly with V_{screen}, as expected, and there is no saturation of the phosphor screen in this range of the post-acceleration voltage.

V_{MCP}	400 V
V_{SCREEN}	3500 V - 6000 V
λ	121.6 nm
P_{beam}	Not available (MPS setup)
Integration times	1 s
T	15 °C

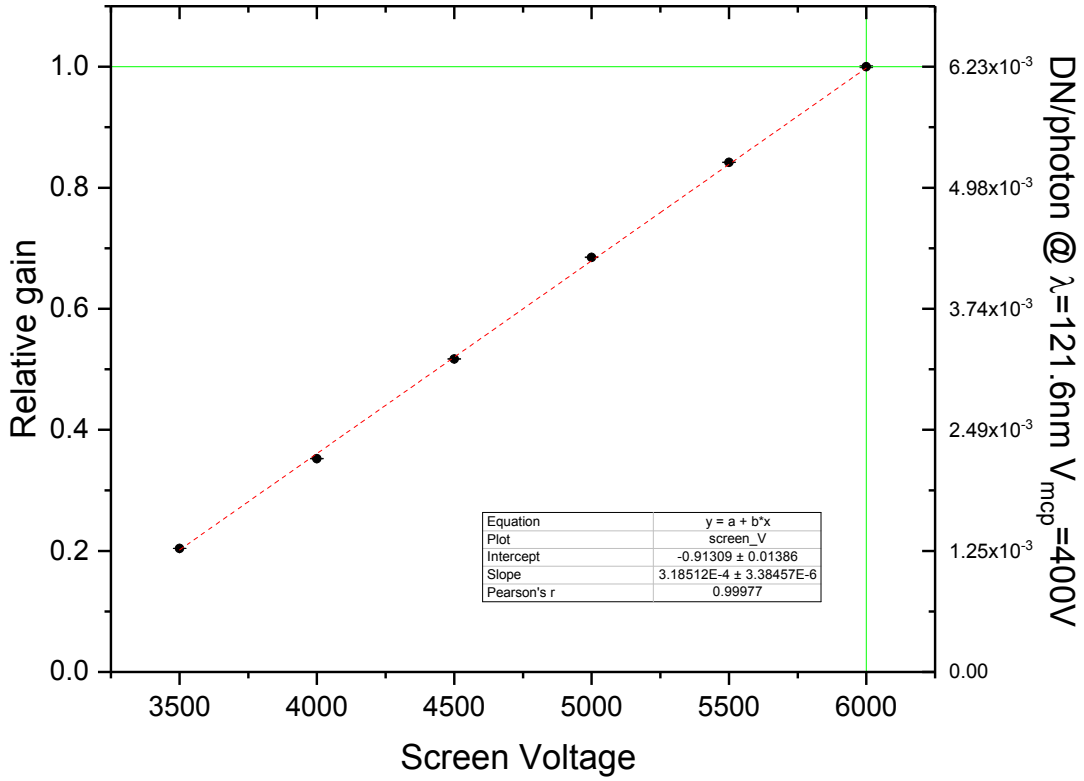

Figure 11. Relative gain vs Screen voltage. The MCP voltage was set to 400 V.

3.5 Response uniformity

The efficiency has been measured at 121.6 nm on a 7x7 grid over the field of view, to measure the response uniformity.

V_{MCP}	500 V
V_{SCREEN}	6000 V
λ	121.6 nm
P_{beam}	188-214 pW
Integration times	1s
T	-20°C

For each point, 40 frames, 1s exposure, have been acquired, corrected for bias and dark and then averaged. During the run, the beam flux has been monitored with a calibrated photodiode and the data have been corrected for the beam flux slightly decreasing during the measurements (~12% from start to the end of the run).

The grid is shown in Figure 12. The relative efficiency (normalized to the maximum value) is shown in Figure 13 with a blue color scale (efficiency grows from dark blue to white). The values in % (with the computed errors) are detailed in Table 7.

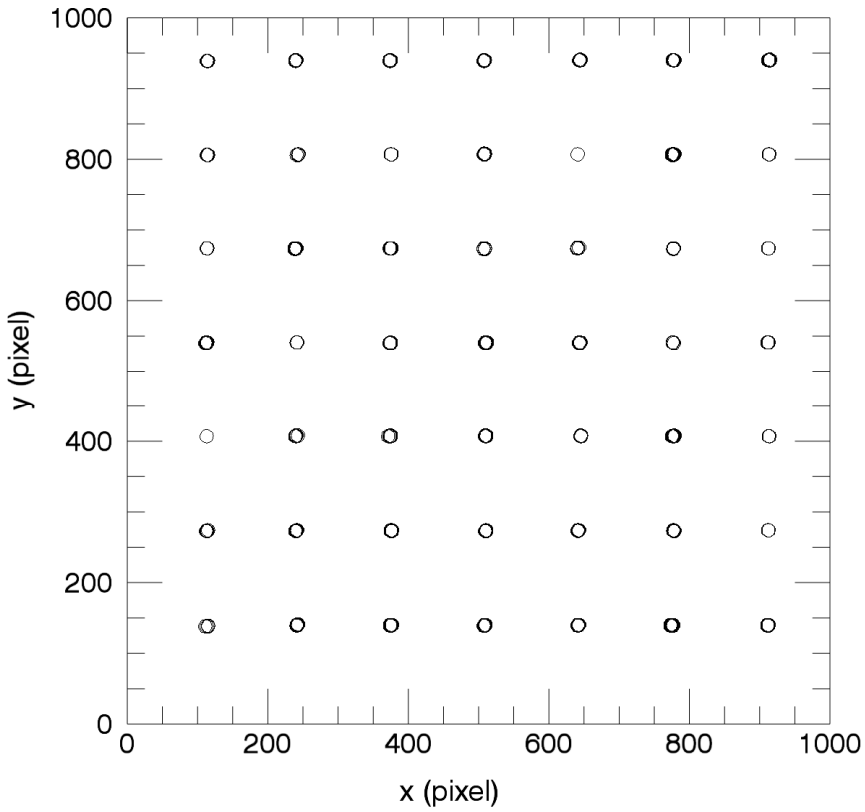

Figure 12. Grid of the measurements

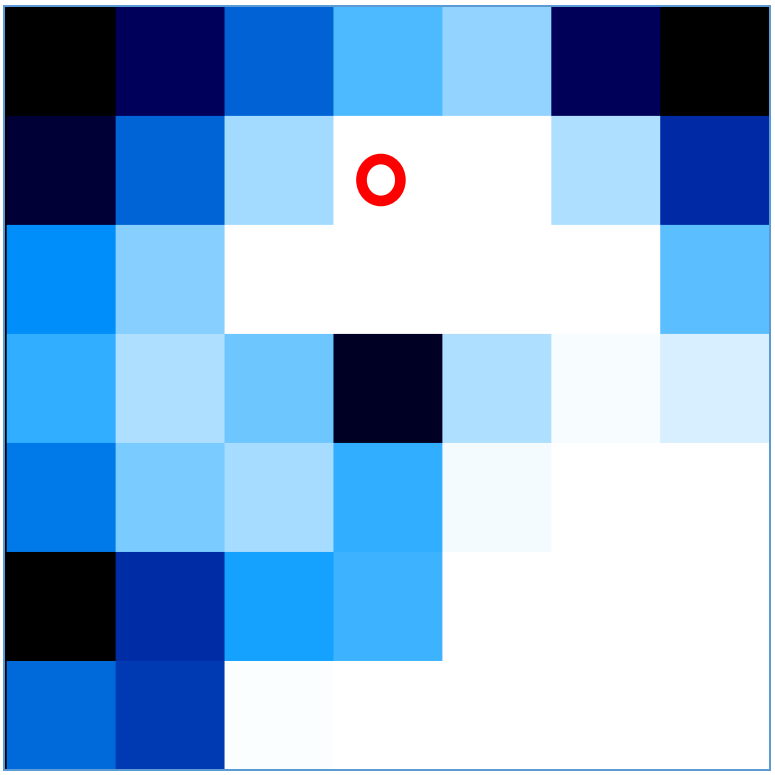

Figure 13. 2D map of the efficiency (increasing from dark blue to white). Position 0,0 is at the lower-left corner. The red circle marks the position of the beam during spectral calibration measurements.

Table 1: Efficiency in % normalized to the maximum.

y \ x	114	242	374	508	641	775	912
939	61.9±1.5	70.3±2.6	76.9±2.5	82.4±3.1	84.4±2.8	70.3±1.5	62.8±2.3
806	68.7±1.6	77.1±2.5	84.8±3.0	88.8±2.9	96.5±3.3	85.2±2.4	74.0±2.3
674	79.6±3.9	84.0±3.3	91.3±2.5	96.7±2.2	98.9±2.7	89.6±2.9	82.7±2.8
540	81.5±4.0	85.2±3.5	83.4±1.9	68.0±0.9	85.3±2.6	87.7±3.0	86.5±3.0
407	78.3±3.3	83.7±3.1	85.1±2.9	81.5±1.1	87.5±3.0	89.8±3.6	88.9±4.4
273	64.5±0.6	74.2±1.5	80.9±2.1	81.8±1.6	90.9±2.4	92.6±3.1	92.7±4.3
138	77.4±4.5	74.8±2.0	87.8±5.4	97.7±9.0	100.0±9.1	98.6±8.9	93.7±7.3

The peak-to-peak variation is around 40%, with the minimum efficiency at two corners, which is not surprising. The rms is 9.5%. More unexpected is the lower-than-average efficiency close to the center of the frame, which is not in agreement with the Lyman-α flat field acquired before. Further investigations carried out at MPS after this test suggested a loss of efficiency due to burn-in of the beam spot in selected regions. The reason is incomplete scrubbing of the MCP, which could not be finalized before the measurements at PTB due to schedule constraints.

4. SUMMARY AND CONCLUSION

The UVDA FM has been characterized before being integrated in Metis. In particular, the detector response as a function of the wavelength, temperature, voltages applied to the intensifier has been measured, along with the linearity of the signal as a function of the exposure time and incident flux. Preliminary results have been reported. Further analysis will be carried out, in particular to characterize in detail the detector non-linearity and the photon counting operative mode.

ACKNOWLEDGMENTS

The authors wish to thank the PTB staff, in particular Alexander Gottwald, Roman M. Klein, Udo Kroth for their support of the measurements at the MLS facility.

The development of the UV camera electronic system has been financed by the Deutsches Zentrum für Luft- und Raumfahrt (DLR). A contribution from the Italian Space Agency (ASI) through the "ASI-INAF agreement I/013/12/0" contract is gratefully acknowledged.

REFERENCES

[1] Müller, D., et al., "Solar Orbiter - Exploring the Sun–Heliosphere Connection", Solar Physics, Vol. 285, 25-70, (2013)

[2] Antonucci, E., et al., "Multi Element Telescope for Imaging and Spectroscopy (METIS) coronagraph for the Solar Orbiter", Proc. SPIE 8443, 844309-12, (2012)

[3] Fineschi S., et al “Novel space coronagraphs: METIS, a flexible optical design for multi-wavelength imaging and spectroscopy,” Proc. SPIE 8862, Solar Physics and Space Weather Instrumentation V, 88620G; doi:10.1117/12.2028544 (2013).
[4] CMOSIS Image Sensors, http://www.cmosis.com/
[5] Piqueras, J., et al., “CMOS sensor and camera for the PHI instrument on board Solar Orbiter: evaluation of the radiation tolerance”, Proc. SPIE 8453, doi:10.1117/12.925403 (2012).
[6] Uslenghi, M., et al., “A prototype of the UV detector for METIS on Solar Orbiter”, Proc. SPIE 8443, (2012)
[7] Bergamini, P., et al., " A fast readout and processing electronics for photon counting intensified charge-coupled device", Review of Scientific Instruments", Volume 71, Issue 4, pp. 1841-1848 (2000)
[8] Uslenghi, M., et al., "Progress on Photon Counting Intensified APS", Proc. SPIE, 4854, pp. 583-592 (2003)
[9] Fraser, G.W., Pearson J.F., Smith G.C., IEEE Trans. Nucl. Sci. Ns-30, 455, (1983)
[10] NOIS1SM1000A datasheet, ON Semiconductor, Rev. 9, August 2011
[11] Reichel, T., et al., Space Telescopes and Instrumentation 2016: Ultraviolet to Gamma Ray, Proc. SPIE 9905, 990547, doi: 10.1117/12.2231405, (2016)